INTERNATIONAL CENTER FOR NUMERICAL METHODS IN ENGINEERING

Lift Maximization with Uncertainties for High Lift Devices Optimization

Z. Tang
J. Périaux
G. Bugeda
E. Oñate

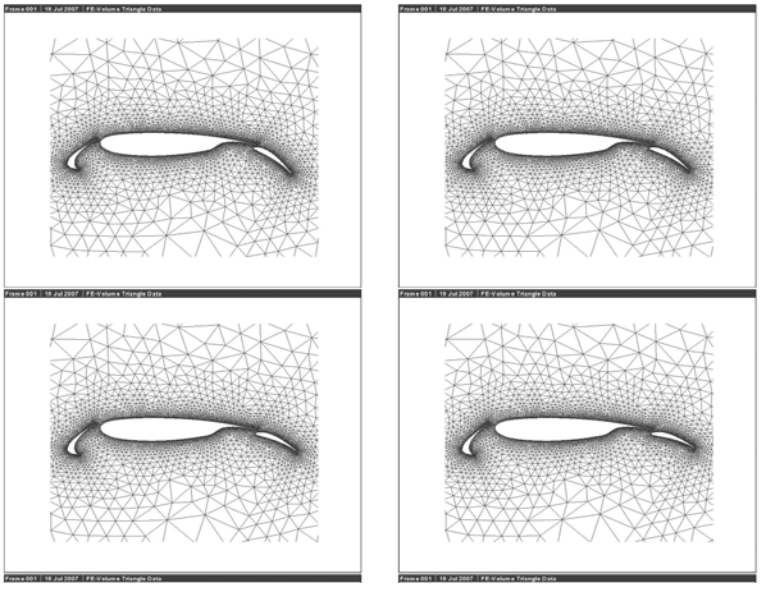

Publication CIMNE Nº-312, October 2008

Lift Maximization with Uncertainties for High Lift Devices Optimization

Z. Tang
J. Périaux
G. Bugeda
E. Oñate

Publication CIMNE Nº-322, October 2008

International Center for Numerical Methods in Engineering
Gran Capitán s/n, 08034 Barcelona, Spain

Lift Maximization with Uncertainties for High Lift Devices Optimization

Z. Tang [a,b] J. Périaux [b] G. Bugeda [b,*] E. Oñate [b]

[a] *College of Aerospace Engineering, Nanjing University of Aeronautics and Astronautics, Nanjing, China*

[b] *Centre Internacional de Métodes Numérics en Enginyeria, Universitat Politécnica Catalunya, Barcelona, Spain*

Abstract

In this paper, the aerodynamic shape optimization problems with uncertain operating conditions has been addressed. After a review of robust control theory and the possible approaches to take into account uncertainties, the use of Taguchi robust design methods in order to overcome single point design problems in Aerodynamics is proposed. Under the Taguchi concept, a design with uncertainties is converted into an optimization problem with two objectives which are the mean performance and its variance, so that the solutions are as less sensitive to the uncertainty of the input parameters as possible. Furthermore, the Multi-Criterion Evolutionary Algorithms (MCEAs) are used to capture a set of compromised solutions (Pareto front) between these two objectives. The flow field is analyzed by Navier-Stokes computation using an unstructured mesh. The proposed approach drives to the solution of a multi-objective optimization problem that is solved using a modification of a Non-dominated Sorting Genetic Algorithm (NSGA). In order to reduce the number of expensive evaluations of the fitness function a Response Surface Modeling (RSM) is employed to estimate the fitness value using the polynomial approximation model. During the solution of the optimization problem a Semi-torsional Spring Analogy is used for the adaption of the computational mesh to all the obtained geometrical configurations. The proposed approach is applied to the robust optimization of the 2D high lift devices of a business aircraft by maximizing the mean and minimizing the variance of the lift coefficients with uncertain free-stream angle of attack at landing and takeoff flight conditions, respectively.

Key words: Design with Uncertainties, Taguchi Methods, Lift Maximization, Evolutionary Algorithms, Semi-Torsional Spring Analogy, Response Surface Modeling

1 Introduction

In spite of the important effect of operating- and manufacturing-uncertainties on the performance, traditional aerodynamic shape optimization has focused on obtaining the best design given a set of deterministic flow conditions. Clearly, it is important to maintain near-optimal performance levels at off-design operating conditions, and to ensure that performance does not degrade appreciably when the component shape differs from the optimal one due to manufacturing tolerances and normal wear and tear. These requirements naturally lead to the idea of robust optimal design wherein the concept of robustness in front of different perturbations is built into the design optimization procedure.

The recognition of the importance of incorporating the probabilistic nature of the variables involved in designing and operating complex systems has led to several investigations in the recent past. Some of the basic principles of robust optimal design are discussed by Egorov et al.[1]. They make the observations that a) robust design optimization is in essence multi-objective design optimization because of the presence of the additional objective (robustness) and, b) the addition of the robustness criterion may result in an optimal solution that is substantially different from that obtained without this criterion. Different approaches to robust optimal design are also mentioned in this paper.

The main objective of this paper is to develop a robust aerodynamic optimization scheme for achieving consistent improvements of the performance over a given range of uncertainty parameters. This scheme has the following two major advantages: (a) it prevents severe degradation in the off-design performance, and (b) it is not sensitive to the number of design points.

The imposition of the additional requirement of robustness results in a multiple-objective optimization problem requiring appropriate solution procedures. Typically the costs associated with multiple-objective optimization are relevant. Therefore, efficient multiple-objective optimization procedures are crucial for the rapid deployment of the principles of robust design in industry. Here, we focus on the applications of an evolutionary algorithm for multiple-objective optimization [2] by using Pareto front concept. Applications of this evolutionary method to some difficult model problems involving the complexities (convex, non-convex, discrete or discontinuous Pareto Front) are also presented in Ref.[2]. The computed Pareto-optimal solutions closely approximate the global Pareto-front and exhibit good solution diversity. Many of these solutions were

* Corresponding author: Gabriel Bugeda
Email address: bugeda@cimne.upc.edu (E. Oñate).
[1] This work was completed with the partial support of National Science Foundation of China under grant number NSFC-10372040.

obtained with relatively small population sizes.

The final goal of this study is to propose an algorithm to take into account the uncertainties related with fluctuating operating conditions integrating them into an automatic shape optimization problem in aerodynamics. We propose to use Taguchi robust design methods in order to overcome single point design problems. The latter techniques produce solutions that perform well for the selected design point but have poor off-design performance. Under the Taguchi concept, a design with uncertainties is converted into an optimization problem with two objectives which are mean performance and its variance, so that the solutions are as less insensitive to the uncertainty of the input parameters as possible. Furthermore, the Multi-Criterion Evolutionary Algorithms (MCEAs) are used to capture a set of compromised solutions (Pareto front) between these two objectives. The flow field is analyzed by Navier-Stokes computation. In order to reduce the number of expensive evaluations of fitness function, Response Surface Modeling (RSM) is employed to estimate fitness value using the approximate model. During the solution of the optimization problem a Semi-torsional Spring Analogy is used to adapt a single computational mesh to all geometrical configurations obtained during the optimization process. The proposed approach is applied to the robust optimization of the 2D high lift devices of a business aircraft, by maximizing the mean and minimizing the variance of the lift coefficients under uncertain free-stream angle of attack at landing and takeoff flight conditions respectively

2 Robust Control and Taguchi Methodology

Many products are now routinely designed with the aid of computer models. Given the inputs designable engineering parameters and the parameters representing manufacturing process conditions the model generates the product's quality characteristics. The quality improvement problem is to choose the designable engineering parameters such that the quality characteristics are uniformly good in the presence of variability of different conditions.

We consider objective functions of the form $f : X \otimes B \longrightarrow \Re$, where $x \in X$ represents decision variables, inputs (designs) controlled by the engineer, $b \in B$ represents uncertainty, inputs not controlled by the engineer, and $f(x, b)$ quantifies the loss suffered by design x under the uncertain conditions b.

Our (unattainable) goal is to find $x^* \in X$ such that, for every $b \in B$,

$$f(x^*, b) \leq f(x, b) \quad \forall x \in X \tag{1}$$

The unsolvable problem of finding $x^* \in X$ that simultaneously minimizes

$f(x, b)$ for each $b \in B$ is the central problem of statistical decision theory: and a decision rule that simultaneously minimizes risk for every possible state of nature. A standard way (e.g., Ferguson[3]) of negotiating this problem is to replace each $f(x, \cdot)$ with a real-valued attribute of it, e.g.,

Minimax Principle :

$$\min_{x \in X} \phi(x), \quad where \;\; \phi(x) = \sup_{b \in B} f(x; b). \tag{2}$$

Bayes Principle :

$$\min_{x \in X} \phi(x), \quad where \;\; \phi(x) = \int_B f(x, b) p(b) db \tag{3}$$

where p denotes a probability density function on B.

The *minimax* principle is extremely conservative. It seeks to protect the decision-maker against the worst-case scenario. The Bayes principle seeks to minimize average loss in a way that can be customized (via the choice of p) to the application. This formulation of the quality control problem was first proposed by Welch, Yu, Kang, and Sacks[4], although their suggestion appears to have had little effect on engineering practice.

Although the above formulation and proposed solution of the quality improvement problem is modern, the problem itself predates the engineering community's use of computer models. To motivate our own approach to this problem, and the more general robust design problem, we briefly summarize the contributions of G. Taguchi. See Roy[5] for a broader context and more detailed discussion of Taguchi's far-ranging contributions to quality engineering.

In the statistical approach, one consider the fluctuating operating conditions $\mathbf{b} = (b_i)_{i=1,\ldots,N}$ as samples of random variables $\mathbf{B} = (B_i)_{i=1,\ldots,N}$, whose statistical characteristics are known (mean $\mu_{\mathbf{B}} = (\mu_B^i)_{i=1,\ldots,N}$, variance $\sigma_{\mathbf{B}}^{\mathbf{2}} = (\sigma_B^{2\,i})_{i=1,\ldots,N}$, etc). One also suppose, for the sake of simplicity, that the random variables $(B_i)_{i=1,\ldots,N}$ are independent. The statistical characteristics of operating conditions can be determined by experimental measurements or engineering experience. Gaussian Probability Density Functions (PDFs) or truncated Gaussian PDFs are often used in practice (see [6] for instance).

The main consequence of this assumption is that the cost function of the problem is also a random variable f. According to the Von Neumann-Morgenstern decision theory, the best choice is then to select the design which leads to the best expected fitness. This is known as the Maximum Expected Values

(MEV) criterion. The decision or design that minimizes the risk is known as the *Bayes' decision* and is solution of the following problem:

$$Minimize\ \mu_f = \int\limits_{\Omega(B)} f(x,b)\rho_B(b)db, \quad x \in \Re^n, \tag{4}$$

$\Omega(B)$ and ρ_B are the range and the PDF of the random variable B. Then, the MEV criterion just consists in minimizing the statistical mean μ_f of the cost function.

This approach is a significant improvement over previous methods. The robust design problem is now considered with a rigorous statistical framework. This allows to take into account the random fluctuations of the fitness in the optimization problem, but also to take care about the frequency of the occurrence of the events, thanks to PDFs. Then, the most probable events have a larger influence in the decision than extreme and unlikely events.

However, problem (4) does not address the variability of the fitness. The mean value of the fitness is the only criterion that is considered in the *Bayes' decision*. For engineering problems, one also would like to select a design for which the fitness is not subjected to large variations when operating conditions fluctuate. Then, a second criterion is often joined to the MEV criterion that relies on the minimization of the variance σ_f^2 of the fitness:

$$Minimize \begin{cases} \mu_f = \int\limits_{\Omega(B)} f(x,b)\rho_B(b)db \\ \sigma_f^2 = \int\limits_{\Omega(B)} (f(x,b)-\mu_f)^2\rho_B(b)db \end{cases} X \in \Re^n, \tag{5}$$

This approach aims at determining a trade-off between the expected fitness and the expected fitness variation as operating conditions randomly fluctuate. Although this approach is satisfactory from theoretical and practical viewpoints, its application is not straightforward. Particularly, the estimation of the mean and variance can be tedious for complex CFD applications. This issue is detailed below. To estimate the mean and variance of the random variable f, one can simply use statistical estimators in a classical Monte-Carlo approach. A sample of operating conditions $(b_i)_{i=1,\ldots,N}$ if size N is generated according to the PDF ρ_B. Then, unbiased estimators of the mean and variance

are:

$$\begin{aligned} \mathbf{M}_f &= \frac{1}{N}\sum_{i=1}^{N} f(x, b_i), \\ S_f^2 &= \frac{1}{N-1}\sum_{i=1}^{N}(f(x, b_i) - \mathbf{M}_f)^2. \end{aligned} \tag{6}$$

This approach does not suffer from *point-optimization effect* since the sample $(b_i)_{i=1,\ldots,N}$ is generated randomly according to the PDF ρ_B.

3 Multi-Objective GAs

The approach described in the previous section drives to the solution of a multi-objective optimization problem. The test cases presented in this work have been solved using a modification of a Non-dominated Sorting Genetic Algorithm (NSGA).

There exist several variants of GAs for multi-objective optimization problems; see for example Vector Evaluated GAs (VEGAs)[7] and Non-dominated Sorting GAs (NSGAs)[8]. For further information on GAs for multi-objective optimization see Reference [9] and references therein. In the following, we describe the basic ideas of NSGA.

The fitness values are computed using the following procedure:

ALGORITHM: Non-dominated Sorting

Choose a large dummy fitness value F;

repeat

Find the non-dominated individuals among the individuals whose fitness values are not set;

Set the fitness value of individuals found in previous step to F;

Decrease the dummy fitness value;

until (fitness values of all individuals are set)

The GAs used is based on NSGA. Since our key idea is to employ the *tournament selection*, it is necessary to make some modifications. The fitness values

are computed exactly in the same way as in NSGA. For each tournament, a fixed number of individuals are selected randomly. The individual which has the highest fitness value wins the tournament, i.e., it is selected to be a parent in the breeding. If there are several such individuals then the first one to enter the tournament wins.

Unfortunately, if there were no modifications to the previous tournament selection, the population would usually converge towards one point on the set of Pareto optimal solutions whereas the aim was to obtain several points from the Pareto set. Therefore, some kind of mechanism is required in order to maintain diversity in population. The most obvious way would be to use the fitness value sharing. It has been shown that this approach fails to preserve the diversity in population [10]. Therefore, a modified algorithm is proposed.

Instead of using any of the previously considered methods, we employ a new way to preserve the diversity of the population. We shall call this approach a tournament slot sharing. A sharing function is defined by

$$Sh(d_{ij}) = \begin{cases} 1 - \left(\dfrac{d_{ij}}{\sigma_{share}}\right)^2, if \;\; d_{ij} < \sigma_{share} \\ \\ 0, \qquad\qquad otherwise, \end{cases} \tag{7}$$

where d_{ij} is the genotypic distance between the individuals i and j, i.e., in our case the Euclidean distance between the vectors defining the designs i and j. The parameter σ_{share} is the maximum sharing distance for a tournament slot. This very same sharing function $Sh(d_{ij})$ is also used in the classical fitness value sharing. Now, the probability for the individual i to enter a tournament is computed using the formula

$$p_i = \frac{1/\sum_{j=1}^{n} Sh(d_{ij})}{\sum_{k=1}^{n}(1/\sum_{j=1}^{n} Sh(d_{ij}))} \tag{8}$$

where the parameter n is the size of population. Hence, this is the same as the roulette wheel selection for the rivals in a tournament. Each individual's slice of roulette wheel is proportional to the inverse of the sum of all sharing functions associated to this individual.

An elitist mechanism is added to our algorithm since it guarantees the cost function values to decrease monotonically from one generation to the next. Also, it usually accelerates the convergence. This is implemented by copying from the old population to the new population all the individuals which would be non-dominated in the new population. Hence, the number of copied individuals varies from one generation to another. For coding, we have used the

floating point coding [11]. This is a rather natural choice, since the design is defined by a vector of floating point numbers. The crossover is made using one crossover site.

The mutation uses a special distribution promoting small mutations. More precisely, the mutation is performed in the following way for a single string: the floating point numbers of the string under consideration are gone through one by one. Let us assume that x is one of these numbers and it is to be mutated. Let l and u be the lower and upper limits for x. The mutated x is denoted by x_m and it is computed as follows:

1. Set $t = (x - l)/(u - l)$;

2. Compute

$$t_m = \begin{cases} t - t\left(\dfrac{t - rnd}{t}\right)^p, & rnd < t, \\ t, & rnd = t, \\ t + (1 - t)\left(\dfrac{rnd - t}{1 - t}\right)^p, & rnd > t \end{cases} \tag{9}$$

where rnd is a random number from the closed interval $[0, 1]$;

3. Set $x_m = (1 - t_m)l + t_m u$.

In step 2, the parameter p defines the distribution of the mutation. We call this parameter the mutation exponent. If $p = 1$ then the mutation is uniform. The probability of small mutations grows as the value of p grows. Hence, we are ready to present the following GA and the parent selection procedure:

ALGORITHM: The Modified NSGA

Initialize population:

Compute object functions (in parallel);

do $i = 2, number - of - generations$

Compute fitness values using non-dominated sorting;

Compute probabilities for each individual to enter tournament;

repeat

Select two parents;

Form two children using crossover;

until (new population is full);

Perform mutation;

Compute object functions (in parallel);

Copy individuals from old population according to elitism;

enddo

ALGORITHM: Select Parent

repeat

Select one individual to tournament using the probabilities p_i in (8);

until (tournament is full);

Find best the individual from the tournament according to the fitness values.

Since about fifteen years ago, Genetic Algorithms have been introduced in aerodynamics shape design problems (see [12] [13][14]. The main concern related to the use of genetic algorithms is the computational effort needed for the accurate evaluation of a configuration that might lead to unacceptable computer time if compared with more classical algorithms. Eventhough, fitness function value can be effectively estimated by using an approximated Response Surface Modeling.

4 2D NS Solver on Unstructured Mesh

In the examples shown at the end of this paper we have solved the 2D Navier-Stokes equations by using a Finite-Volume Galerkin method on unstructured meshes. A 2D unstructured mesh has been generated by the pre/post-processing software **GID** of CIMNE. To solve the Euler part of the equations, a Roe scheme has been used. To compute turbulent flows a $k - \varepsilon$ model has been chosen. Near-wall turbulence has been computed by a two-layer approach. Time dependant problems have been solved using a fourth order Runge-Kutta scheme.

5 Response Surface Modeling Methods[15]

One of the most important advantages obtained by using response surface models in optimization is a significant reduction in the computational cost. This allows the user to perform global optimization and reliability-based optimization, which are otherwise prohibitively computationally expensive. In addition, the use of response surface models allows the design engineer to quickly perform a variety of trade-off studies which provide information about the sensitivity of the optimal aircraft design with respect to changes in performance criteria and to off-design conditions.

The reduction in the computational cost of optimization provided by response surface models motivates their use in the modeling of data, despite the fact that, under certain conditions, they can produce some numerical noise.

In many RSM applications, either linear or quadratic polynomials are assumed to accurately model the observed response values. If n_s analysis are performed and $p = 1, ..., n_s$, then a quadratic response surface (RS) model has the form

$$y^{(p)} = c_0 + \sum_{1 \le j \le n_v} c_j x_j^{(p)} + \sum_{1 \le j \le k \le n_v} c_{(n_v - 1 + j + k)} x_j^{(p)} x_k^{(p)}, \tag{10}$$

where $y^{(p)}$ is the response; $x_j^{(p)}$ and $x_k^{(p)}$ are the n_v design variables; and c_0, c_j, and $c_(n_v - 1 + j + k)$ are the unknown polynomial coefficients. Note that there are $n_t = (n_v + 1)(n_v + 2)/2$ coefficients (i.e., model terms) in the quadratic polynomial. This polynomial model may be written in matrix notation as

$$y^{(p)} = C^T \bar{X}^{(p)}, \tag{11}$$

where C is the vector of length n_t of unknown coefficients to be estimated,

$$C = [c_0, c_1, ..., c_{n_t - 1}], \tag{12}$$

and $\bar{X}^(p)$ is the vector of length n_t corresponding to the form of the $x_j^{(p)}$ and $x_k^{(p)}$ terms in the polynomial model (10). For the p^{th} observation this is

$$\bar{X}^{(p)} = [1, x_1^{(p)}, x_2^{(p)}, ...x_{n_v}^{(p)}, (x_1^{(p)})^2, x_1^{(p)} x_2^{(p)}, ..., (x_{n_v}^{(p)})^2]. \tag{13}$$

Note that there is a difference between the p^{th} vector of independent variables, $X^{(p)}$, and the p^{th} vector of independent variables mapped into the form of the polynomial model, $\bar{X}^{(p)}$.

Estimating the unknown coefficients requires n_s analysis, where $n_s \geq n_t$. Under such conditions, the estimation problem may be formulated in matrix notation as

$$Y \approx XC, \tag{14}$$

where Y is the vector of n_s observed response values,

$$Y = [y^{(1)}, y^{(2)}, ..., y^{(n_s)}], \tag{15}$$

and X is the matrix formed by the n_s row vectors $\bar{X}^{(p)}$ which is assumed to have rank n_t. Thus, X may be expressed as

$$X = \begin{bmatrix} 1 & x_1^{(1)} & x_2^{(1)} & \dots & (x_{n_v}^{(1)})^2 \\ \vdots & \vdots & \vdots & \ddots & \vdots \\ 1 & x_1^{(n_s)} & x_2^{(n_s)} & \dots & (x_{n_v}^{(n_s)})^2 \end{bmatrix}. \tag{16}$$

The unique least squares solution to Equation (14) is

$$\hat{C} = \left(X^T X\right)^{-1} X^T Y, \tag{17}$$

where $\left(X^T X\right)^{-1}$ exists if the rows of X are linearly independent. When C is substituted by $\hat{C}$ into Equation (11), values of the response may be predicted at any location $\mathbf{x}$ by mapping $\mathbf{x}$ into $\bar{X}^{(p)}$. In matrix notation this corresponds to

$$\hat{Y} = \hat{C}^T \bar{X}^{(p)}. \tag{18}$$

Note that if $n_s > n_t$ the system of equations is overdetermined. Thus, the predicted response values (from the polynomial model) at the original sample locations may differ from the observed response values at the sampled locations.

Polynomial RS models can be considered as *global* models in which all of the n_s observed values of the response are equally weighted in the fitting of the polynomial surface. At an unsampled location in design space, $\mathbf{x}$, response observations that are near to $\mathbf{x}$ (in the sense of Euclidean distance) have an equal influence on the predicted response, $\hat{f}(\mathbf{x})$, as the response observations that are far from $\mathbf{x}$. It can be argued that such a global model may not be

the best approximation if the true unknown response has many real local optima (as opposed to the artificial local optima created by numerical noise). In such a situation an approximation scheme having *local* modelling properties may be more attractive, i.e., where $\hat{f}(\mathbf{x})$ is more strongly influenced by nearby measured response values and is less strongly influenced by those further away. Such local modelling behavior is characteristic of interpolation models, for which DACE models are one particular implementation.

6 Semi-torsional Spring Analogy for Mesh Movement

During any shape optimization process there is a need for a simple, robust and computationally efficient scheme for maintaining element quality during mesh deformation. This can be provided by a spring analogy approach. This scheme must work in both 2D and 3D, be able to handle large deformations, and work well for fully unstructured meshes. Paper [16] presented such a scheme, developed as an extension of the 2D semi-torsional approach. We have used it in our optimization approach to perform 2D Multi-element unstructured mesh movement due to slat/flap position modifications. This has allowed to use the same computational mesh for all the different computational geometries obtained during the solution of the optimization problem.

6.1 Lineal spring analogy

Spring analogy models consist in considering the mesh as an assembly of springs with a given stiffness for each one. Each of the edges of the mesh is considered as a spring. Then, after the modification of the geometry of the boundary, the new resulting mesh is obtained as the new equilibrated position of the springs network.

The lineal spring stiffness k_{ij} for a given element edge $i-j$ takes the following general form:

$$k_{ij}^n = \frac{\lambda}{[(y_{1,i}^n - y_{1,j}^n)^2 + (y_{2,i}^n - y_{2,j}^n)^2 + (y_{3,i}^n - y_{3,j}^n)^2]^\beta}, \tag{19}$$

where the superscript n denotes time step, $(y_{1,i}^n, y_{2,i}^n, y_{3,i}^n)$ and $(y_{1,j}^n, y_{2,j}^n, y_{3,j}^n)$ are the spatial coordinates of the two nodes connected by the edge $i-j$ at time step n, and λ and β are coefficients. The fictitious spring force $\overrightarrow{F}_{ij}^n$ acting on node i from edge $i-j$ is

$$\overrightarrow{F}_{ij}^n = k_{ij}^n(\overrightarrow{\delta}_j^n - \overrightarrow{\delta}_i^n), \tag{20}$$

where $\overrightarrow{\delta}^n_j$ and $\overrightarrow{\delta}^n_i$ are nodal displacements of node j and i at step n respectively. The static equilibrium equation for node i at time step n is

$$\sum_{j=1}^{NE_i} k_{ij}^n \left(\overrightarrow{\delta}^n_j - \overrightarrow{\delta}^n_i \right) = 0, \tag{21}$$

where N_{ei} is the number of nodes directly connected to node i through fictitious springs. A system of equations is derived by applying the equilibrium equation to all nodes in the mesh. Nodal coordinates are updated by adding the nodal displacements to the old coordinates:

$$\overrightarrow{y}^n_i = \overrightarrow{y}^{n-1}_i + \overrightarrow{\delta}^n_i. \tag{22}$$

The coefficient β is often taken to be $0,5$, which means that the stiffness is inversely proportional to the length of the edge, and $\lambda = 1$.

6.2 Semi-torsional spring analogy

A semi-torsional spring analogy model is similar to the lineal formulation, with angle information incorporated into the spring stiffness. Neither displacement formulation nor force transformation is needed, and this approach is therefore easy to implement[16]. For 2D triangular elements, a semi-torsional stiffness of an edge $i - j$ was proposed by Blom [17].

$$k_{ij}^{semi-torsional} = \frac{k_{ij}^{lineal}}{\theta}, \tag{23}$$

where θ is the angle facing the edge on an element. However, this semi-torsional model is not directly applicable to 3D elements. Moreover, an internal edge in a 2D triangular mesh is attached to two elements, and faces two angles which are usually different in magnitude. The above definition gives different stiffness values to a single edge when it is considered on each of its two attached elements.

To deform 2D/3D unstructured meshes for solving moving boundary problems, we propose a semi-torsional spring analogy model based on Zeng's previous work [16], in which the stiffness of an edge is defined as the sum of its linear stiffness and its semi-torsional stiffness, with the semi-torsional stiffness

depending on the angle facing the edge, i.e.

$$\begin{aligned} k_{ij} &= k_{ij}^{lineal} + k_{ij}^{semi-torsional} \\ k_{ij}^{semi-torsional} &= k \sum_{m=1}^{NE_{ij}} \frac{1}{sin^2\theta_m^{ij}} \end{aligned} \tag{24}$$

where the lineal stiffness is defined as in Eq. (19), NE_{ij} is the number of elements sharing edge $i-j$, and θ_m^{ij} is the facing angle, defined as the angle that faces the edge $i-j$ on the mth element attached to the edge. k is a coefficient having the dimension of the stiffness. In all our numerical experiments, we set the value of the coefficient to be $1,0$. On a tetrahedron with vertices i, j, k and l, the angle that faces the edge $i-j$ is taken as the angle formed between triangle $\triangle^{ikl}$ and triangle $\triangle^{jkl}$.

By substituting (24) into (20), the spring forces on nodes i and j are expressed as

$$[F_{ij}] = \left(\frac{\lambda}{l_{ij}} + k \sum_{m=1}^{NE_{ij}} \frac{1}{sin^2\theta_m^{ij}} \right) [B] \, [u_{ij}] \, , \tag{25}$$

where $[F_{ij}] = [F_{ix}, F_{iy}, F_{iz}, F_{jx}, F_{jy}, F_{jz}]^T$, $[u_{ij}] = [u_i, v_i, w_i, u_j, v_j, w_j]^T$ are vectors of spring forces and displacements at nodes i and j , $[B]$ is a 6×6 matrix whose elements are given by $B_{pq} = -\delta_{pq} + \delta_{p,q+3} + \delta_{p+3,q}$, with $\delta_{pq} = 1$ if $p = q$ and $\delta_{pq} = 0$ if $p \neq q$.

For a 2D triangular mesh one edge within the mesh shares two elements and Eq. (24) simplifies to

$$k_{ij}^{semi-torsional} = k \left(\frac{1}{sin^2\theta_1} + \frac{1}{sin^2\theta_2} \right) , \tag{26}$$

where θ_1 is the angle facing edge $i-j$ on the triangle $\triangle_{ijl}$, θ_2 is the angle facing edge $i-j$ on $\triangle_{ijk}$ and k, l, i and j are the vertices of the elements.

In a 2D triangular mesh, spring forces on the edge $i-j$ are

$$[F_{ij}] = \left(\frac{\lambda}{l_{ij}} + k \left(\frac{1}{sin^2\theta_1} + \frac{1}{sin^2\theta_2} \right) \right) [B^*] \, [u_{ij}] \, , \tag{27}$$

where $[F_{ij}] = [F_{ix}, F_{iy}, F_{jx}, F_{jy}]^T$, $[u_{ij}] = [u_i, v_i, u_j, v_j]^T$, and $[B^*]$ is a 4×4 matrix whose elements are given by $B^*_{pq} = -\delta_{pq} + \delta_{p,q+2} + \delta_{p+2,q}$.

With the above definition for semi-torsional stiffness, an angle approaching 0 or π makes the edge facing this angle very stiff, which prevents further change in the angle and thus avoids element inversion.

6.3 Boundary improvement

Since the static equilibrium equations for the mesh are elliptic, the principle of Saint Venant holds for deformation of the mesh. Therefore, boundary displacement does not spread far into the mesh. A boundary-improvement technique was suggested to handle this localization of deformation [19]. The stiffness of springs adjacent to the boundary was increased so that surface displacement could be spread further into the mesh. To implement this, the coefficient λ is magnified by a constant factor for springs adjacent to the boundary.

Several layers of elements near the boundary can be made stiffer by this boundary improvement technique. In our experiments, we imposed one layer of boundary stiffness modification by increasing λ from 1,0 to 3,5.

Some additional techniques to improve this situation can be seen in [27].

6.4 Mesh Testing Results

We have implemented the semi-torsional model for 2D multi element airfoil geometries with slat and flap movement, see Figure 1. In this example, the main-body of an airfoil is fixed and the position and the orientation of slat and flap are modified. Then, the interior mesh is modified by using above analogy methods according to the boundary displacement. Figure 1 shows the mesh movement provided for different positions of slat and flat.

7 Application to High Lift Device Optimization

In order to test the proposed approach the robust optimization of a high lift device has been faced. The goal of the optimization is to maximize C_l or $\frac{C_l}{C_d}$ at landing or takeoff fly conditions by modifying the positions and orientations of slat and flap. The aerodynamic coefficients are computed using N-S flow solver. Here the design variables are the positions (2 coordinates for each one) and angles of slat and flap, so that we have six design variables in total.

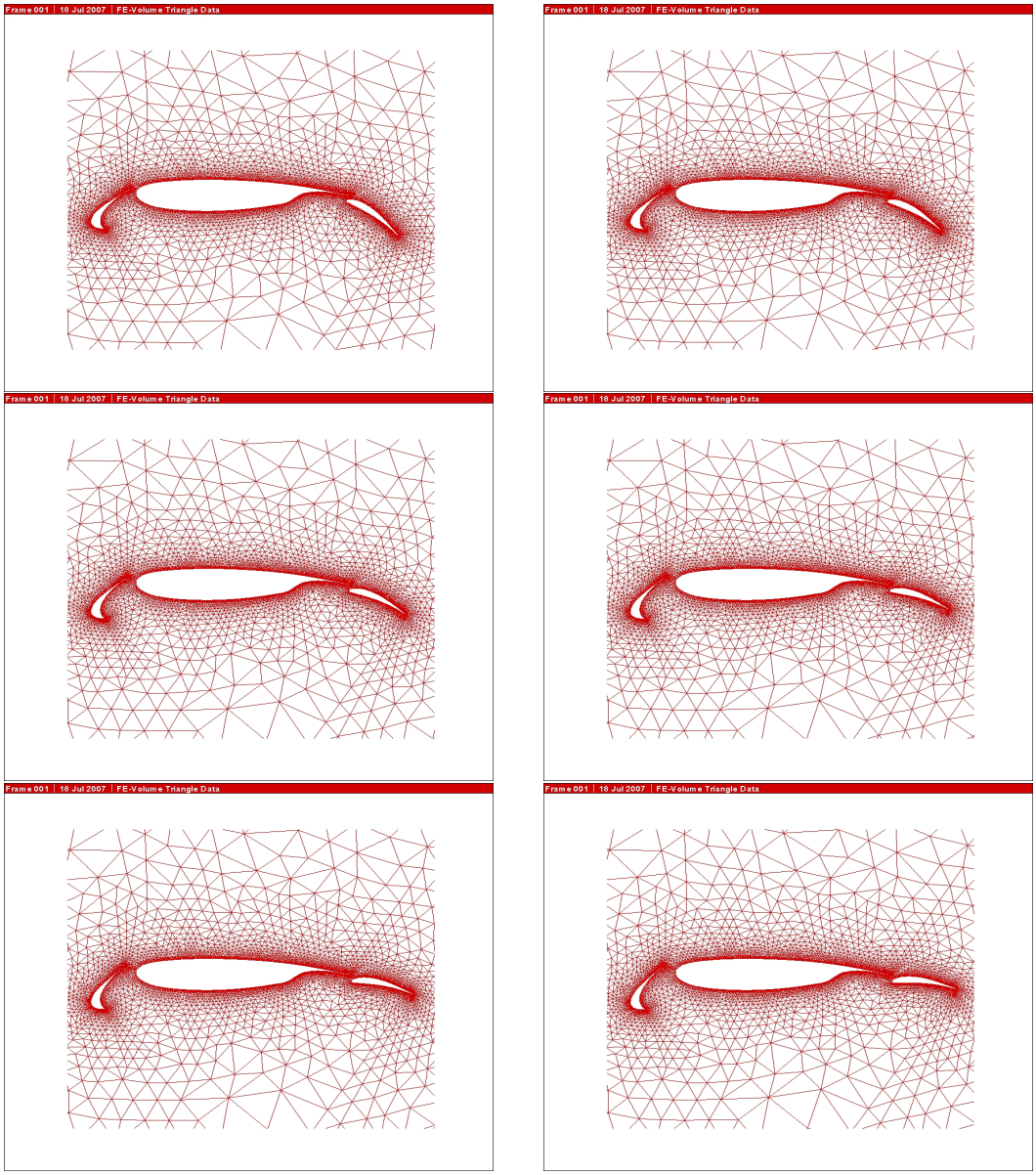

Fig. 1. Example of 2D springs methods for unstructured mesh movement. Mesh movement provided for different positions of slat and flat.

7.1 Single-point Lift Maximization at Landing Flight Condition

For landing configurations, we only concern about the maximum lift, because in this situation drag is considered as convenient. So that, the optimization problem is defined as

$$\max C_l \tag{28}$$

The nominal operating condition is defined for landing conditions by the free-stream incidence $\alpha = 15^0$, Mach number $M_\infty = 0,15$ and Reynolds number $Re = 1,8 \times 10^6$.

Figure 2 shows the convergence history of lift coefficient obtained during the optimization process. The optimized airfoil slat and flap positions are shown in Figure 3 compared with the baseline multi element airfoil. Red one shows the optimized airfoil positions and blue one is the baseline airfoil. The optimized pressure distribution is shown in Figure 4. Again, red points show the pressure distribution on optimized airfoil and blue ones show baseline pressure distribution. Table 1 gives the detailed evolution of the lift coefficient value during the optimization process.

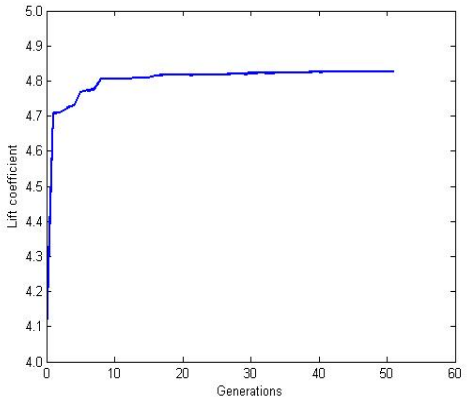

Fig. 2. Convergence history of lift coefficient

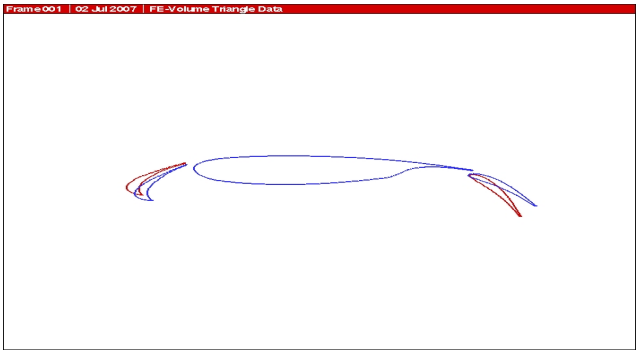

Fig. 3. Optimized multi element airfoil configuration for landing

Table 1
Lift coefficient values during optimization

Generations	0	10	20	30	40	50
C_l	4,073	4,805	4,816	4,822	4,825	4,827

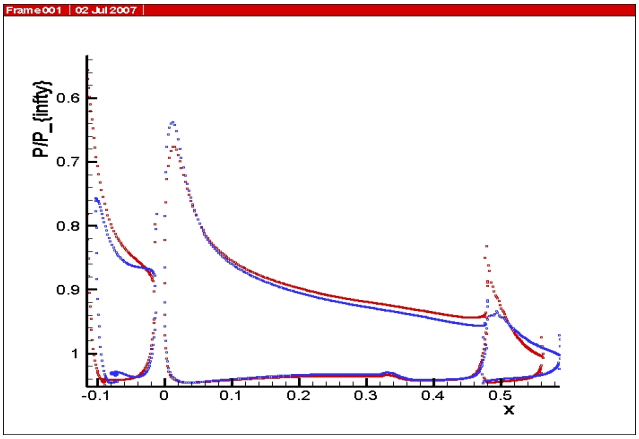

Fig. 4. Comparison of pressure distributions between optimized and baseline for landing

7.2 Single-point Lift Maximization at Takeoff Flight Condition

For takeoff conditions, we not only concern about maximum lift but also about minimum drag. So, the optimization problem is defined as

$$\max \frac{C_l}{C_d} \tag{29}$$

The nominal operating condition are defined for takeoff conditions by the free-stream incidence $\alpha = 8^0$, Mach number $M_\infty = 0,15$ and Reynolds number $Re = 1,8 \times 10^6$.

Figure 5 shows the convergence history of the aspect ratio of lift to drag coefficient obtained during the optimization process. The optimized airfoil slat and flap positions are shown in Figure 6 compared with the baseline multi element airfoil. Red one shows the optimized airfoil positions and blue one is the baseline airfoil. Streamlines over optimized multi-element airfoil are shown in Figure 7. It is obviously noticed that there is a vortex behind slat. Table 2 gives the detailed aspect ratio value of lift to drag coefficient obtained during the optimization process.

Table 2
Aspect ratio values of lift to drag coefficient during optimization

Generations	0	10	20	30	40	50
C_l/C_d	22,59	34,13	36,20	36,37	36,51	36,55

By comparing the optimized airfoil configurations of the two above optimization problems we can observe that the flap is more slopping down for landing

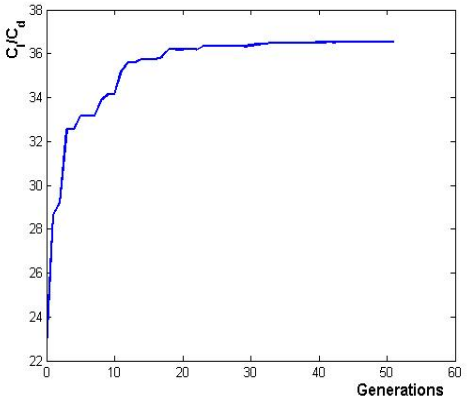

Fig. 5. Convergence history of aspect ratio of lift to drag coefficient

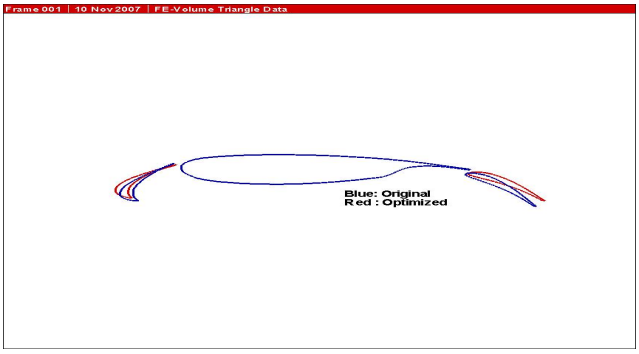

Fig. 6. Optimized multi element airfoil configuration for takeoff

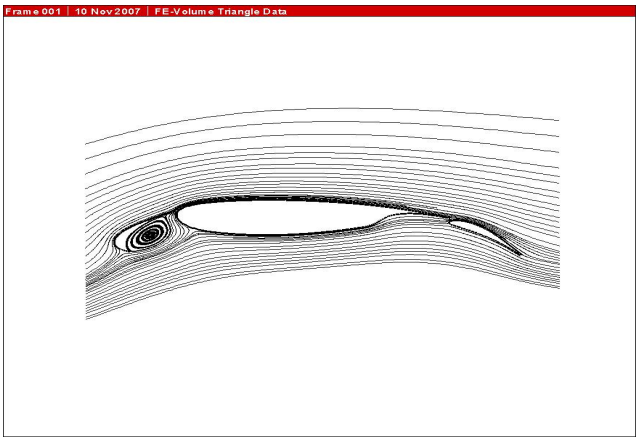

Fig. 7. Streamlines over multi element airfoils optimized for takeoff

than for takeoff. This is due to the fact that both maximum lift and maximum drag are needed for landing, whereas maximum lift and minimum drag are needed for takeoff.

7.3 Lift Maximization With Uncertain Angle of Attack at Landing Flight Condition

In this case we assume that the free-stream angle of attack is subject to random fluctuations. For simplicity, we assume that its PDF is uniform in the interval $[15^0 - 2^0, 15^0 + 2^0]$. The mean angle of attack corresponds to the nominal incidence 15^0. Free-stream Mach number is $M_\infty = 0,15$ and Reynolds number $Re = 1,8 \times 10^6$. The mathematical formulation of the resulting optimization problem is defined as

$$\max C_l \qquad at \;\; M_\infty =, 0, 15, \;\; \alpha = [15^0 - 2^0, 15^0 + 2^0]. \tag{30}$$

According to the Taguchi robust control theory, the above design problem with uncertainties can be converted into the following two-objective optimization problem, one objective is the mean value of the lift coefficient, and the other is the variance of lift coefficient over the range of uncertainty.

$$\begin{cases} \max f_1 = \mu_{C_l} = \dfrac{1}{N}\displaystyle\sum_{i=1}^{N} C_{li} \\ \\ \min f_2 = \sigma_{C_l} = \dfrac{1}{N-1}\displaystyle\sum_{i=1}^{N}(C_{li} - \mu_{C_l})^2 \end{cases} \tag{31}$$

where $N = 5$, $M_\infty = 0,15$ and $\alpha_i = [13^0, 14^0, 15^0, 16^0, 17^0]$. The above two-objective optimization problem is solved via Multi-objective GAs.

Figure 8 shows the compromised Pareto front of the above two-objective optimization problem. Figure 9 illustrates the optimized airfoil slat and flap positions of one solution on pareto front compared with the baseline and traditional one-point optimized shape. Red one shows the robust optimized airfoil positions, blue one is the baseline airfoil and green one is traditional designed airfoil in section 7.1. Stream lines over optimized airfoil are shown in Figure 10. Two clear vortices appear behind the slat and the flap. The optimized pressure distribution is shown in Figure 11. Red points show the pressure distribution on optimized airfoil and blue ones show baseline pressure distribution.

Figure 12 shows a comparison between one of the obtained robust optimized, the traditional single-point optimized and the baseline airfoils. We can see how the lift coefficient of the robust optimized airfoil is not as sensitive as the single-point optimized one to the fluctuation of the angle of attack. This is also illustrated by the value of C_l for the optimized and baseline airfoils in table 3.

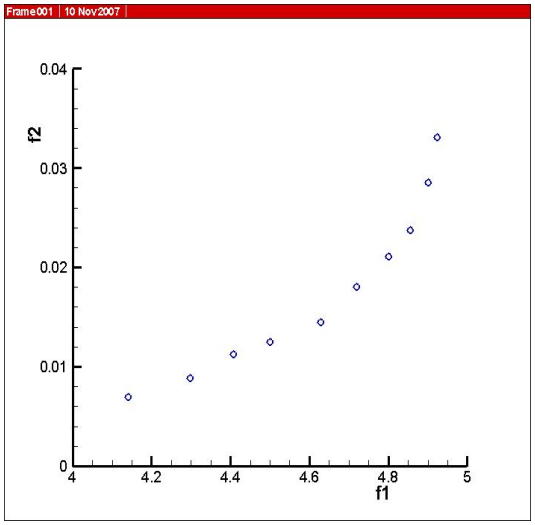

Fig. 8. Pareto front between mean lift and its variance

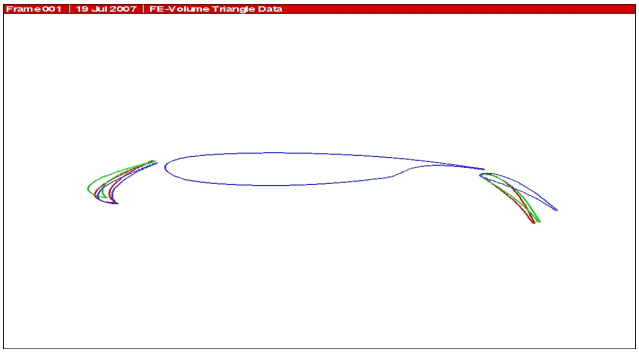

Fig. 9. Robust optimized multi element airfoil configuration for Landing

Fig. 10. Stream lines over the robust optimized airfoil

8 Conclusion

The problem of aerodynamic shape optimization with uncertain operating conditions is addressed in this paper. It is solved by using the Taguchi concept

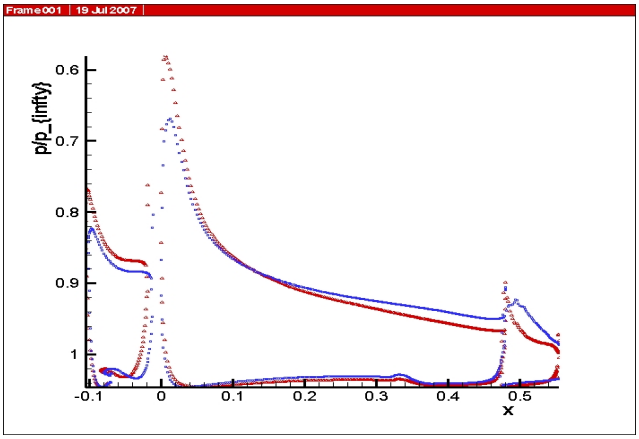

Fig. 11. Comparison of pressure distributions between robust optimized and baseline airfoil for landing

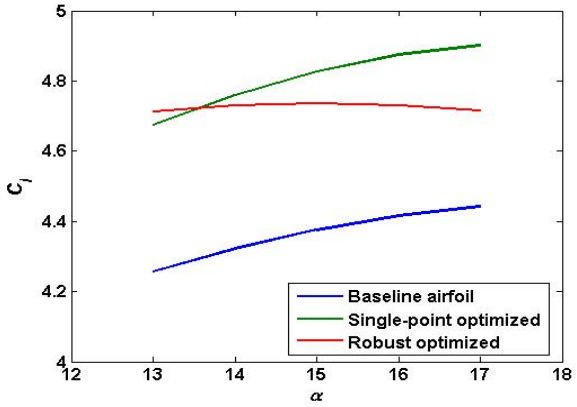

Fig. 12. Comparison of the lift coefficient between robust optimized, traditional single-point optimized and baseline airfoils

converting design with uncertainties into a two-objective optimization problem: one objective is the mean performance, the other one is the variance of the performance. To overcome the difficulty related to the high computational cost required by robust design and GAs, a response surface modeling strategy is proposed that relies on the polynomial approximation, to estimate the fitness value. In addition, a semi-torsional spring analogy is used for the deformation of the computational mesh in order to fit it to the different geometries obtained during the shape optimization process.

This methodology is demonstrated for a realistic high lift device's lift maximization in subsonic flow with fluctuation on free stream incidence angle. This optimization problem is solved using the proposed Taguchi robust control method successfully.

Table 3
Comparison of robust optimized airfoil performances with traditional single-point optimized and baseline ones

	α	13^0	14^0	15^0	16^0	17^0
Baseline Airfoil	C_l	4,2461	4,3220	4,3757	4,4161	4,4427
	C_d	0,1742	0,1837	0,1939	0,2041	0,2147
Optimized (Landing)	C_l	4,6762	4,7596	4,8271	4,8753	4,9015
	C_d	0,2130	0,2224	0,2328	0,2458	0,2602
Robust Optimized (Landing)	C_l	4,7129	4,7302	4,7358	4,7307	4,7155
	C_d	0,2440	0,2540	0,2642	0,2751	0,2870

References

[1] Egorov, I. N.; Kretinin, G. V.; and Leshchenko, I. A. *How to Execute Robust Design*. AIAA Paper No. 2002-5670, 9th AIAA/USAF/NASA/ISSMO Symposium on Multidisciplinary Analysis and Optimization, September 4-6, Atlanta, Georgia, 2002.

[2] Chung, H. and Alonso, J. *Multiobjective Optimization Using Approximation Model Based Genetic Algorithms*. AIAA Paper No. 2004-4325, Tenth AIAA/ISSMO Multidisciplinary Analysis and Optimization Conference, Albany, New York, August 30 C Sep. 1, 2004.

[3] Ferguson, T. S. *Mathematical Statistics: A Decision Theoretic Approach*. Academic Press, New York, 1967.

[4] Welch, W. J.; Yu, T. K.; Kang, S. M.; and Sacks, J. *Computer experiments for quality con- trol by parameter design*. Journal of Quality Technology, 22:15-22, 1990.

[5] Roy, R. K. *A Primer on the Taguchi Method*. Competitive Manufacturing. Van Nostrand reinhold, New York, 1990.

[6] Huyse, L. *Free-form airfoil shape optimization under uncertainty using maximum expected value and second order second-moment strategies*. NASA/CR-2001-211020 or ICASE Report No. 2001-18, 2001.

[7] Schaffer, J. D. *Some experiments in machine learning using vector evaluated genetic algorithms*. TCGA file no.00314, Ph.D thesis, Vanderbilt University, Nashville, TN, 1984.

[8] Srinivas, N. and Dep, K. *Multiobjective optimization using nondominated sorting in genetic algorithms*. Evolutionary Computing, 3, 221-248, 1995.

[9] Mäkinen, R. A.; Toivanen, J. and Periaux, J. *Multidisciplinary Shape Optimization in Aerodynamics and Electromagnetics using Genetic Algorithms*, International Journal for Numerical Methods in Fluids, Volume 30, Issue 2, Pages 149- 159, 1999.

[10] Mäkinen, R. A. E. and Toivanen, J. *Parallel solution of optimal shape design problem governed by Helmholtz/potential flow equations*. in D. H. Bailey et al. (eds), The 7th SIAM Conference on Parallel Processing for Scientific Computing, SIAM, 102-103, 1995.

[11] Michalewicz, Z. *Genetic algorithms + data structures = evolution programs*. Springer-Verlag, 1992.

[12] Périaux, J.; Sefrioui, M.; Stouflet, B.; Mantel, B.; Laporte, E. *Robust genetic algorithms for optimization problems in aerodynamic design*. Genetic algorithms in engineering and computer science, John Wiley & Sons, pp. 397-415, 1995.

[13] Quagliarella, D. *Genetic algorithms applications in computational uid dynamics, Genetic algorithms in engineering and computer science*. John Wiley & Sons, pp. 417-442 1995.

[14] Spendley, W.; Hext, GR.; Himsworth, FR. *Sequential application of simplex designs in optimization and evolutionary operation*. Technometrics 4 (1962), 441-461, 1962.

[15] Giunta, A. A.; Narducci, R.; Burgee, S.; Grossman, B.; Mason, W. H.; Watson, L. T.; and Haftka, R. T. *Variable-Complexity Response Surface Aerodynamic Design of an HSCT Wing*. in Proceedings of the 13th AIAA Applied Aerodynamics Conference, pp. 994-1002, San Diego, CA, AIAA Paper 95-1886, June, 1995.

[16] Zeng, D.; Ethiera, C. R. *A semi-torsional spring analogy model for updating unstructured meshes in 3D moving domains*. Finite Elements in Analysis and Design, Vol. 41, pp1118-1139, 2005.

[17] Blom, F. J. *Considerations on the spring analogy*. Int. J. Numer. Methods Fluids 32. 647, 2000.

[18] Farhat, C.; Degand, C.; Koobus, B.; Lesoinne, M. *Torsional springs for two-dimensional dynamic unstructured fluid meshes*. Comput. Methods Appl. Mech. Eng. 163. 231, 1998.

[19] Blom, F. J.; Leyland, P. *Analysis of fluid-structure interaction by means of dynamic unstructured meshes*. J. Fluids Eng. -Trans. ASME 120. 792, 1998.

[20] Tang, Z. L.; Périaux, J.; Désidéri, J. A. *Multi Criteria Robust Design Using Adjoint Methods and Game Strategies For Solving Drag Optimization Problems With Uncertainties*. West-East High Speed Flow Field Conference (WEHSFF05), Beijing, October, 19-22, 2005.

[21] Duvigneau, R. *Aerodynamic Shape Optimization with Uncertain Operating Conditions using Metamodels*. INRIA report RR-6143, 2007.

[22] Zingg, D. and Elias, S. *Aerodynamic Optimization Under a range of operating conditions*. AIAA Journal. 44, 11, 2787-2791, 2006.

[23] Hirt, C. W.; Nichols, B. D. *Volume of fluid (Vof) method for the dynamics of free boundaries*. J. Comput. Phys. 39, 201, 1981.

[24] Batina, J. T. *Unsteady Euler airfoil solutions using unstructured dynamic meshes*. AIAA J. 28. 1381, 1990.

[25] Degand, C.; Farhat, C. *A three-dimensional torsional spring analogy method for unstructured dynamic meshes*. Comput. Struct. 80. 305, 2002.

[26] Bugeda, G.; Ródenas, J. J.; Oñate, E. *An Integration of a Low Cost Adaptive remeshing Strategy in The Solution of Structural Shape Optimization Problems Using Evolutionary Methods*. Comput. Struct., Vol. 86, 1563–1578, 2008.

[27] Chiandussi, G.; Bugeda, G.; Oñate, E. *A simple method for automatic update of finite element meshes*. Communications in Numerical Methods in Engineering, Vol. 16, 1–19, 2000.